

# Photon tunneling through absorbing dielectric barriers

Toralf Gruner and Dirk-Gunnar Welsch  
Friedrich-Schiller-Universität Jena, Theoretisch-Physikalisches Institut  
Max-Wien Platz 1, D-07743 Jena, Germany

## Abstract

Using a recently developed formalism of quantization of radiation in the presence of absorbing dielectric bodies, the problem of photon tunneling through absorbing barriers is studied. The multilayer barriers are described in terms of multistep complex permittivities in the frequency domain which satisfy the Kramers-Kronig relations. From the resulting input-output relations it is shown that losses in the layers may considerably change the photon tunneling times observed in two-photon interference experiments. It is further shown that for sufficiently large numbers of layers interference fringes are observed that cannot be related to a single traversal time.

PACS number(s): 42.50.Ct, 73.40.Gk, 42.79.-e

# 1 Introduction

Stimulated by recent experiments [1, 2, 3], the problem of photon tunneling through multilayer dielectric barriers has been of increasing interest. In order to answer the question of what is the time that is spent by a photon inside such a barrier, the effects of dispersion and absorption should be considered very carefully. The calculations that have been performed so far are based on real refractive indices of the layers [1, 2, 3, 4], so that a number of questions, such as the influence of absorption on the measured traversal times [5], have been open. It is well known that in frequency intervals where the dielectric layers are nearly transparent the action of each layer and hence that of a multilayer barrier can be described in terms of unitary transformations that relate the operators of the outgoing fields to those of the incoming fields (see, e.g., Ref. [6]). These input–output relations and the underlying quantization scheme (see, e.g., Refs. [7, 8, 9]) of course fail, when the effects of absorption cannot be disregarded.

Various approaches to the problem of quantization of radiation in the presence of absorbing dielectric bodies have been developed [10, 11, 12, 13, 14, 15, 16, 17, 18, 19, 20, 21]. In the present paper we use the quantization scheme given in Refs. [20, 21]. It is based on a Green function expansion of the operator of the (transverse) vector potential and applies to radiation in both homogeneous and inhomogeneous dielectric matter. In this approach, the matter is described in terms of a complex permittivity (in the frequency domain), without using a particular microscopic model for the matter. The only condition is that the permittivity satisfies the Kramers–Kronig relations, because of causality. Applying the method to the calculation of input–output relations for radiation at absorbing multilayer dielectric barriers, we can systematically study the effects of dispersion and absorption on the propagation of single-photon wave packets through such barriers.

The paper is organized as follows. In Sec. 2 the quantization scheme is outlined. In Sec. 3 the scheme is applied to radiation falling on multilayer dielectric barriers. The input–output relations derived are used in Sec. 4 in order to calculate barrier traversal times measurable in two-photon interference experiments. Finally, a summary is given in Sec. 5.

## 2 Field quantization

Let us consider linearly polarized light propagating in  $x$  direction in an inhomogeneous linear dielectric medium. Introducing the (transverse) vector potential

$$A(x, t) = \int_0^\infty d\omega e^{-i\omega t} A(x, \omega) + \text{c.c.} \quad (1)$$

( $A \equiv A_y$ ), the classical (phenomenological) Maxwell equations yield

$$\left[ \frac{\partial^2}{\partial x^2} + \frac{\omega^2}{c^2} \epsilon(x, \omega) \right] A(x, \omega) = 0, \quad (2)$$

where

$$\epsilon(x, \omega) = \epsilon_r(x, \omega) + i \epsilon_i(x, \omega) \quad (3)$$

is the complex permittivity which for inhomogeneous media, such as multilayer dielectric barriers, varies with  $x$ . Clearly, when the permittivity is complex, then Eq. (2) cannot be valid as an operator equation in quantum theory. On the other hand, it is well known that propagation of light in absorbing matter is unavoidably accompanied by noise. In a quantized version of Eq. (2) this noise source can be taken into account by introducing an operator noise current  $\hat{j}_n$ , so that [21]

$$\left[ \frac{\partial^2}{\partial x^2} + \frac{\omega^2}{c^2} \epsilon(x, \omega) \right] \hat{A}(x, \omega) = \hat{j}_n(x, \omega), \quad (4)$$

where

$$\hat{j}_n(x, \omega) = \frac{\omega}{c^2} \sqrt{\frac{\hbar}{\pi \epsilon_0 \mathcal{A}}} \epsilon_i(x, \omega) \hat{f}(x, \omega). \quad (5)$$

Here,  $\hat{f}(x, \omega)$  is a bosonic basic field,

$$[\hat{f}(x, \omega), \hat{f}^\dagger(x', \omega')] = \delta(x - x') \delta(\omega - \omega'), \quad (6)$$

$$[\hat{f}(x, \omega), \hat{f}(x', \omega')] = [\hat{f}^\dagger(x, \omega), \hat{f}^\dagger(x', \omega')] = 0, \quad (7)$$

and  $\mathcal{A}$  is a normalization area in the  $yz$  plane. Equation (4) is now an equation for the the (Schrödinger) operator  $\hat{A}(x, \omega)$ . The solution can be represented as

$$\hat{A}(x, \omega) = \int dx' G(x, x', \omega) \hat{j}_n(x', \omega), \quad (8)$$

where  $G(x, x', \omega)$  is the classical Green function that satisfies the equation

$$\left[ \frac{\partial^2}{\partial x^2} + \frac{\omega^2}{c^2} \epsilon(x, \omega) \right] G(x, x', \omega) = \delta(x - x') \quad (9)$$

and vanishes in the limit when  $x \rightarrow \pm\infty$ . The quantization scheme ensures that the well-known equal-time commutation relation

$$[\hat{A}(x, t), \hat{E}(x', t)] = -\frac{i\hbar}{\mathcal{A}\epsilon_0} \delta(x - x') \quad (10)$$

is preserved [21].

### 3 Input–output relations

Let us consider a dielectric barrier consisting of  $(N - 2)$  layers ( $N \geq 3$ ),

$$\epsilon(x, \omega) = \sum_{j=1}^N \lambda_j(x) \epsilon_j(\omega), \quad (11)$$

where  $\epsilon_j(\omega)$  is the permittivity of the  $j$ th layer, and

$$\lambda_j(x) = \begin{cases} 1 & \text{if } x_{j-1} < x < x_j, \\ 0 & \text{otherwise} \end{cases} \quad (12)$$

( $x_0 \rightarrow -\infty, x_N \rightarrow \infty$ ). From Eqs. (1), (8), and (9), with  $\epsilon(x, \omega)$  from Eq. (11), the operator  $\hat{A}(x, \omega)$  can be rewritten as [21]

$$\begin{aligned} \hat{A}(x) = & \sum_{j=1}^N \lambda_j(x) \int_0^\infty d\omega \sqrt{\frac{\hbar \beta_j(\omega)}{4\pi c \omega \epsilon_0 \epsilon_j(\omega) \mathcal{A}}} \\ & \times \left[ e^{i\beta_j(\omega)\omega x/c} \hat{a}_{j+}(x, \omega) + e^{-i\beta_j(\omega)\omega x/c} \hat{a}_{j-}(x, \omega) \right] + \text{H.c.}, \quad (13) \end{aligned}$$

where the quasi-mode operators  $\hat{a}_{j+}(x, \omega)$  and  $\hat{a}_{j-}(x, \omega)$ , which are associated with the (damped) waves propagating to the right and left, respectively, are related to the bosonic basic field as

$$\begin{aligned} \hat{a}_{j\pm}(x, \omega) = & \hat{a}_{j\pm}(x', \omega) e^{\mp\gamma_j(\omega)\omega(x-x')/c} \\ & \pm \frac{1}{i} \sqrt{2\gamma_j(\omega) \frac{\omega}{c}} \int_{x'}^x dy e^{\mp\gamma_j(\omega)\omega(x-y)/c} e^{\mp i\beta_j(\omega)\omega y/c} \hat{f}(y, \omega) \quad (14) \end{aligned}$$

( $x_{j-1} \leq x, x' \leq x_j$ ). Here the notation  $\sqrt{\epsilon_j(\omega)} = n_j(\omega) = \beta_j(\omega) + i\gamma_j(\omega)$  is introduced.

Using the commutation relation (6), from Eqs. (14) we find that the quasi-mode operators  $\hat{a}_{1+}(x, \omega)$ ,  $x \leq x_1$ , and  $\hat{a}_{N-}(x, \omega)$ ,  $x \geq x_N$ , of the incoming radiation from the left and the right, respectively, satisfy the commutation relations

$$\left[ \hat{a}_{1+}(x, \omega), \hat{a}_{1+}^\dagger(x', \omega') \right] = \delta(\omega - \omega') e^{-\gamma_1(\omega)\omega|x-x'|/c}, \quad (15)$$

$$\left[ \hat{a}_{N-}(x, \omega), \hat{a}_{N-}^\dagger(x', \omega') \right] = \delta(\omega - \omega') e^{-\gamma_N(\omega)\omega|x-x'|/c}, \quad (16)$$

$$\left[ \hat{a}_{1+}(x, \omega), \hat{a}_{N-}^\dagger(x', \omega') \right] = 0. \quad (17)$$

Note that Eqs. (15) and (16) agree with the commutation relations valid for the corresponding bulk materials. For vanishing absorption ( $\gamma_{1(N)}(\omega) \rightarrow 0$ ) the operators  $\hat{a}_{1+}$  and  $\hat{a}_{N-}$  are independent of  $x$  and ordinary free-field bosonic operators [21].

The output operators  $\hat{a}_{1-}(x, \omega)$ ,  $x \leq x_1$ , and  $\hat{a}_{N+}(x, \omega)$ ,  $x \geq x_N$ , can then be calculated step by step starting from a single-slab plate ( $N=3$ ). Using Eqs. (13) and (14) and taking into consideration that the vector potential must be continuously

differentiable at the interfaces, after some lengthy calculation we find that the output operators can be expressed in terms of the input operators and bosonic operator noise sources  $\hat{g}_\pm(\omega)$  associated with the losses in the barrier [20, 23],

$$\begin{pmatrix} \hat{a}_{1-}(x_1, \omega) \\ \hat{a}_{N+}(x_{N-1}, \omega) \end{pmatrix} = \tilde{\mathbf{T}}(\omega) \begin{pmatrix} \hat{a}_{1+}(x_1, \omega) \\ \hat{a}_{N-}(x_{N-1}, \omega) \end{pmatrix} + \tilde{\mathbf{A}}(\omega) \begin{pmatrix} \hat{g}_+(\omega) \\ \hat{g}_-(\omega) \end{pmatrix}, \quad (18)$$

$$[\hat{g}_\pm(\omega), \hat{g}_\pm^\dagger(\omega')] = \delta(\omega - \omega') \quad (19)$$

(the input and noise operators are commuting quantities). Here the characteristic transformation matrix  $\tilde{\mathbf{T}}(\omega)$  describes the effects of transmission and reflection of the input fields [22], whereas the losses inside the barrier give rise to an absorption matrix  $\tilde{\mathbf{A}}(\omega)$ . Explicit expressions for the matrices  $\tilde{\mathbf{T}}(\omega)$  and  $\tilde{\mathbf{A}}(\omega)$  and the noise operators  $\hat{g}_\pm(\omega)$  [as linear functionals of the field  $\hat{f}(x, \omega)$  inside the barrier] are given in Ref. [23].

The input–output relations (18) [together with Eq. (14)] lead to commutation relations for the output operators  $\hat{a}_{1-}(x, \omega)$ ,  $x \leq x_1$ , and  $\hat{a}_{N+}(x, \omega)$ ,  $x \geq x_N$ , that differ, in general, from those in Eqs. (15) – (17) for the input operators. The difference decreases with increasing distances from the barrier. In particular, it can be disregarded when the surrounding medium can be regarded as being lossless and the input and output operators are ordinary bosonic operators. In this case the relations

$$\begin{aligned} |T_{11}(\omega)|^2 + |T_{12}(\omega)|^2 + |A_{11}(\omega)|^2 + |A_{12}(\omega)|^2 \\ = |T_{21}(\omega)|^2 + |T_{22}(\omega)|^2 + |A_{21}(\omega)|^2 + |A_{22}(\omega)|^2 = 1, \end{aligned} \quad (20)$$

$$T_{11}(\omega)T_{21}^*(\omega) + T_{12}(\omega)T_{22}^*(\omega) + A_{11}(\omega)A_{21}^*(\omega) + A_{21}(\omega)A_{22}^*(\omega) = 0 \quad (21)$$

can be shown to be valid, which ensure preservation of the bosonic commutation relations.

## 4 Photon tunneling

To study the influence of dispersion and absorption on photon tunneling through multilayer dielectric barriers, let us consider a two-photon experiment of the type described in Ref. [1] (Fig. 1). Pairs of down-conversion photons are directed by mirrors to impinge on the surface of a 50%:50% beam splitter and the output coincidences are measured. One photon (I) of each pair travels through air, while the conjugate photon (II) passes a barrier. The coincidences attain a minimum when the two photons' wavepackets overlap perfectly at the beam splitter. This can be achieved by translating an appropriately chosen prism in one arm of the interferometer in order to compensate for the delay owing to the barrier.

Let us assume that the barrier is in the ground state and the two correlated photons are prepared in the state

$$|\Psi\rangle = \int_0^\infty d\Omega \alpha(\Omega) \int_0^\Omega d\omega f(\omega)f(\Omega - \omega) \hat{a}_I^\dagger(\omega) \hat{a}_{II}^\dagger(\Omega - \omega) |0\rangle, \quad (22)$$

where  $\alpha(\Omega)$  and  $f(\omega)$  are the bandwidth functions of the laser and down-conversion photons, respectively,  $f(\omega)$  being centered at  $\Omega/2$ . From photodetection theory it is well known (see, e.g., [25]) that the overall coincidences  $R$  can be obtained from the time-integrated normally ordered intensity correlation function,

$$R = \xi^2 \int dt_1 \int dt_2 \langle \hat{E}^{(-)}(t_1) \hat{E}^{(-)}(t_2) \hat{E}^{(+)}(t_1) \hat{E}^{(+)}(t_2) \rangle, \quad (23)$$

where  $\hat{E}^{(\pm)}(t_1)$  and  $\hat{E}^{(\pm)}(t_2)$  are the fields at the detectors in the two output channels of the beam splitter ( $\xi$ , detection efficiency). Applying the input–output relations (18) and using Eq. (22), after some lengthy but straightforward calculation we find that

$$R = 2\pi^2 \mathcal{N}^4 \int_0^\infty d\Omega \alpha^2(\Omega) F(\Omega), \quad (24)$$

$$F(\Omega) = \int_0^\Omega d\omega \left| f^2(\omega) f^2(\Omega - \omega) \right| \omega(\Omega - \omega) T_{12}^*(\Omega - \omega) \left[ T_{12}(\Omega - \omega) - e^{-2i\Omega s} e^{4i\omega s} T_{12}(\omega) \right], \quad (25)$$

where  $s$  is the translation length of the prism (cf. Fig. 1), and the abbreviation  $\mathcal{N} = \sqrt{\xi \hbar / (4\pi c \epsilon_0 \mathcal{A})}$  has been introduced.

The translation length  $s = s_0$  that corresponds to the minimum of  $R(s)$  is usually used in order to distinguish between superluminal (positive values of  $s_0$ ) and subluminal behaviour (negative values of  $s_0$ ) of the photon passing through the barrier. In the numerical calculations we have considered  $\text{H(LH)}^k$  structured plates (H, titanium dioxide; L, fused silica) of  $\lambda/4$ -layers, which are of the type described in Ref. [1]. We have calculated the function  $T(\omega)$  applying the algorithm given in Ref. [23]. Due to the lack of reliable data we have assumed that in the (relevant) frequency interval the complex refractive indices are approximately independent of frequency, so that all the dependences on frequency effectively result from the geometry of the barrier. For the sake of simplicity we have assumed that the line shape function of the exciting laser,  $\alpha(\Omega)$ , is sufficiently small, so that  $F(\Omega) \approx F(\omega_0)$  in Eq. (24), where  $\omega_0$  is the centre frequency ( $\omega_0 = 5.37 \times 10^{15} \text{s}^{-1}$ ). Introducing the single-photon pulse shape function  $f(t) = (2\pi)^{-1/2} \int d\omega \exp[-i\omega t] f(\omega)$ , we have performed calculations for both Gaussian pulses  $f(t) \propto \exp[i\omega_0 t/2 - (t/t_0)^2]$  and time-limited non-Gaussian pulses  $f(t) \propto \exp\{i\omega_0 t/2 - [1 - [t/(2t_0)]^2]^{-1}\}$  if  $|t| < 2t_0$  and  $f(t) = 0$  elsewhere, where  $t_0 = 20 \text{ fs}$  in either case.

The values of  $\Delta\tau = 2s_0/c$  that are shown in Fig. 2 are valid for both Gaussian and time-limited non-Gaussian pulse shape functions. The values are positive and indicate superluminal behaviour of the photon at the barrier, the characteristic tunneling time being given by  $\tau_t = l/c - \Delta\tau$  ( $l$ , thickness of the barrier). From the figure we see that the “lead” of the photon,  $\Delta\tau$ , increases with the number of layers of the barrier,  $N = 2k + 1$ , and tends to a linear function of  $N$ , the slope of which sensitively depends on the losses in the barrier. Disregarding the losses, the slope in the linear regime is simply given by the inverse velocity of light in vacuum, which indicates that  $\tau_t$  is

independent of  $N$ . The effect of losses is seen to decrease the slope which implies that  $\tau_t$  is increased.

The interval of  $N$  in which  $\Delta\tau$  (linearly) increases with  $N$  must of course be limited by an upper boundary, which may substantially change with the pulse shape function of the photon at the entrance plane. For the system under consideration the increase of  $\Delta\tau$  with  $N$  ends when  $N \approx 35$  (lossless case) or  $N \approx 41$  (lossy case) for the time-limited non-Gaussian pulse, whereas for the Gaussian pulse the boundary value of  $N$  is substantially increased. It should be pointed out that the observed increase of  $\Delta\tau$  with  $N$  is not in contradiction to causality. The effect can simply be explained by a shift of the pulse maximum towards earlier times owing to pulse reshaping in the barrier, where the earliest time is given by the time at which the pulse starts from zero. Since in the case of a Gaussian pulse the pulse maximum can be shifted to earlier times than in the case of a time-limited pulse, in the former case the upper boundary of  $N$  is higher than in the latter case.

For sufficiently large  $N$  the introduction of the time  $\tau$  (and the traversal time  $\tau_t$ ) makes little sense. In Fig. 3 the transmittance of the barrier,  $T_{12}(\omega)$ , is plotted for relatively low (11) and high (41) numbers of layers. Since the spectral line shape function of the outgoing photon,  $\bar{f}(\omega) \propto f(\omega)T_{12}(\omega)$ , sensitively depends on the two competing quantities  $f(\omega)$  and  $T_{12}(\omega)$  (Figs. 4, 5), it can essentially be different from that of the incoming photon when the number of layers is large enough (compare Fig. 4 with Fig. 5). The behaviour in the time domain is illustrated in Figs. 6 and 7 in which the intensity of the outgoing photon,  $\bar{I}(t) = \langle \hat{E}^{(-)} \hat{E}^{(+)} \rangle$ , is plotted. In particular, for sufficiently large  $N$  the incoming and outgoing photons' wavepackets lose all resemblance to each other (cf. Figs. 5 and 7). In this case the measured coincidences are expected to be more or less complicated functions of the translation length, the structure of which does not allow one to define uniquely a traversal time.

Figures 4 – 7 refer to the case when the pulse of the incoming photon is time-limited. Compared to such a pulse, the spectral line shape function  $f(\omega)$  of a Gaussian pulse is more smoothed and its wings decrease substantially faster. Hence, the transformed line shape function  $f(\omega)T_{12}(\omega)$  of a Gaussian pulse reflects the frequency response of the transmittance of the barrier,  $T_{12}(\omega)$ , less sensitively than that of a time-limited non-Gaussian pulse. This different behaviour explains the above mentioned difference in the boundary values of  $N$ .

In Figs. 8 and 9 the coincidences are shown as a function of the translation length for the chosen time-limited pulse shape and various numbers of layers. We clearly see that when the value of  $N$  exceeds an upper boundary value, then the function  $R(s)$  loses the simple structure that can typically be described by a well-defined minimum. It should be noted that, compared to lossless barriers, frequency-selective absorption shifts the boundary towards higher values. With increasing  $N$  interference fringes are observed, which correspond to the various possibilities of (partial) overlapping of the undisturbed and the multi-peaked outgoing photons' wavepackets at the beam splitter. Clearly, each minimum introduces its own characteristic time, and a unique tunneling time can be hardly derived in this way.

## 5 Summary and Conclusions

On the basis of a Green function approach to the problem of quantization of radiation in inhomogeneous, dispersive and absorptive linear dielectrics we have derived quantum optical input-output relations for optical fields at multilayer dielectric plates, which can be regarded as generalizations of the well-known concepts of unitary transformations that apply to non-absorbing matter. Applying the theory to photon tunneling through absorbing barriers, we have shown that relatively small imaginary parts of the refractive indices of the layers can already give rise to observable effects in two-photon interference experiments as performed recently.

The results reveal that only up to an upper boundary for the number of layers the measured coincidences can be used for extracting from them a characteristic time that may be regarded as traversal time. The boundary value sensitively depends on the spectral line shape function of the photon at the barrier and the dependence on frequency of the transmittance of the barrier, which can be substantially different for absorbing and non-absorbing barriers. It is worth noting that for sufficiently large numbers of layers the photon's wavepacket can be distorted in the barrier to such an extent that the observed coincidences show a number of interference fringes which correspond to different time constants.

## Acknowledgement

One of us (T.G.) is grateful to R.Y. Chiao for valuable comments.

## References

- [1] R.Y. Chiao, P.G. Kwiat and A.M. Steinberg, *Quant. Semiclass. Opt.* 7 (1995) 259.
- [2] A.M. Steinberg and R.Y. Chiao, *Phys. Rev. A* 51 (1995) 3525.
- [3] Ch. Spielmann, R. Szipöcs, A. Stingl and F. Krausz, *Phys. Rev. Lett.* 73 (1994) 2308.
- [4] Y. Japha and G. Kurizki, *Phys. Rev. A* 53 (1996) 586.
- [5] A.M. Steinberg, *Phys. Rev. A* 52 (1995) 32.
- [6] L. Knöll, W. Vogel and D.-G. Welsch, *Phys. Rev. A* 42 (1990) 503; *J. Opt. Soc. Am. B* 3 (1986) 1315.
- [7] L. Knöll, W. Vogel and D.-G. Welsch, *Phys. Rev. A* 36 (1987) 3803.
- [8] R.J. Glauber and M. Lewenstein, *Phys. Rev. A* 43 (1991) 467.



- [9] H. Khosravi and R. Loudon, Proc. R. Soc. Lond. Ser. A 433 (1991) 337; *ibid.* 436 (1992) 373.
- [10] M. Fleischhauer and M. Schubert, J. Mod. Opt. 38 (1991) 677.
- [11] G.S. Agarwal, Phys. Rev. A 11 (1975) 230.
- [12] B. Huttner and S.M. Barnett, Europhys. Lett. 18 (1992) 487; Phys. Rev. A 46 (1992) 4306.
- [13] L. Knöll and U. Leonhardt, J. Mod. Opt. 39 (1992) 1253.
- [14] D. Kupiszewska, Phys. Rev. A 46 (1992) 2286.
- [15] S.-T. Ho and P. Kumar, J. Opt. Soc. Am. B 10 (1993) 1620.
- [16] J.R. Jeffers, N. Imoto and R. Loudon, Phys. Rev. A 47 (1993) 3346.
- [17] T. Gruner and D.-G. Welsch, Phys. Rev. A 51 (1995) 3246.
- [18] S.M. Barnett, R. Matloob and R. Loudon, J. Mod. Opt. 42 (1995) 1165.
- [19] R. Matloob, R. Loudon, S.M. Barnett and J. Jeffers, Phys. Rev. A 52 (1995) 4823.
- [20] T. Gruner and D.-G. Welsch, Proceedings of the Third Workshop on Quantum Field Theory under the Influence of External Conditions, Leipzig, 1995 (ed. M. Bordag, B.G. Teubner Verlagsgesellschaft, Stuttgart, Leipzig, 1996).
- [21] T. Gruner and D.-G. Welsch, Phys. Rev. A 53 (1996) 1818.
- [22] M. Born and E. Wolf, Principles of Optics (Pergamon Press, London, 1959).
- [23] T. Gruner and D.-G. Welsch, quant-ph/9511041; Phys. Rev. A, to be published.
- [24] H.R. Philipp, EMIS Datareview, Aug. 1987.
- [25] W. Vogel and D.-G. Welsch, Lectures on Quantum Optics (Akademie Verlag, Berlin 1994).

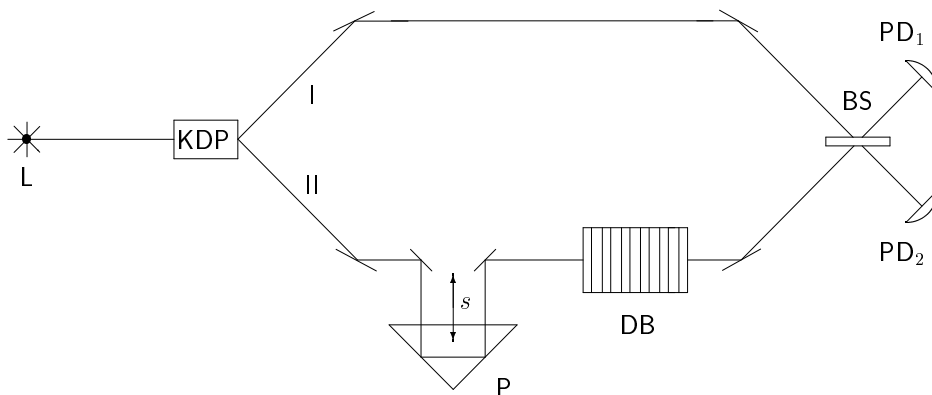


Figure 1: Scheme of the two-photon interference experiment [1, 2] for determining photon traversal times through multilayer dielectric barriers (L, laser; P, prism; DB, dielectric barrier; BS, beam splitter; PD<sub>1</sub>, PD<sub>2</sub>, photodetectors).

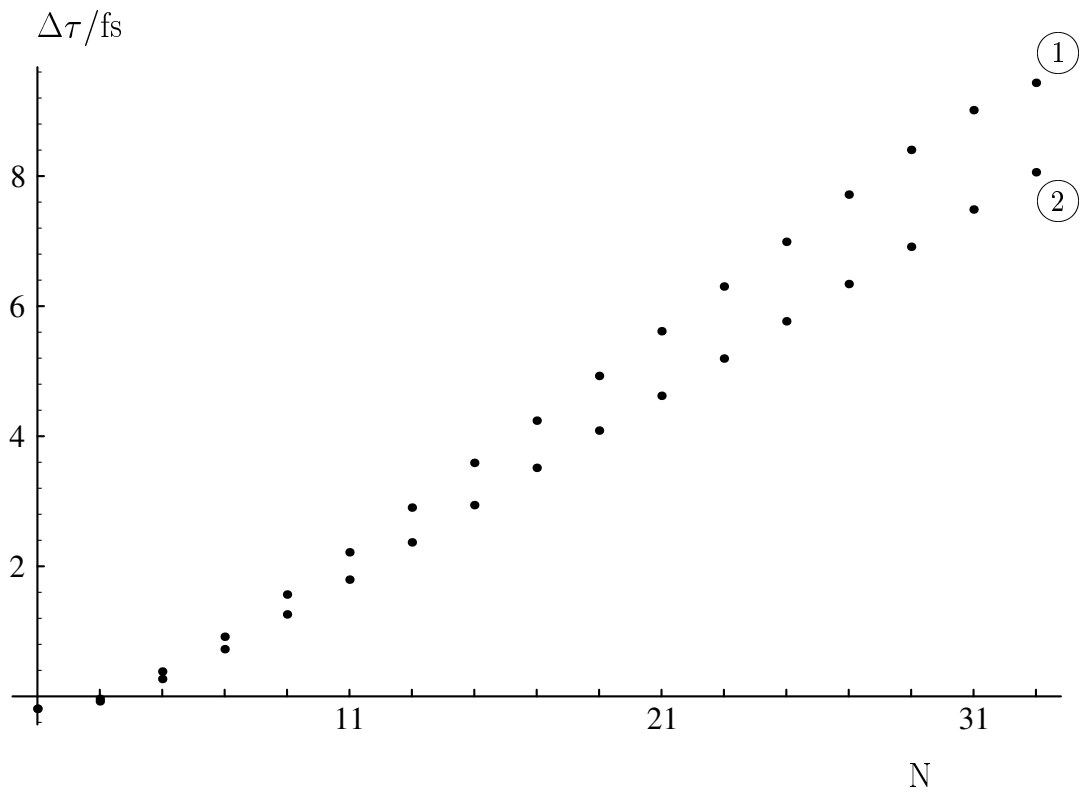


Figure 2: The temporal “lead”  $\Delta\tau = 2s_0/c$  that corresponds to the position  $s_0$  of the minimum of  $R(s)$  is shown as a function of the number of layers,  $N = 2k + 1$ , for a  $H(LH)^k$  structured plate of  $\lambda/4$ -layers of the type described in Ref. [1]; curve (1): lossless barrier ( $n_{\text{TiO}_2} = 2.22$ ,  $n_{\text{SiO}_2} = 1.41$ ), curve (2): absorbing barrier ( $n_{\text{TiO}_2} = 2.22$ ,  $n_{\text{SiO}_2} = 1.41 + 0.0372i$  [24]).

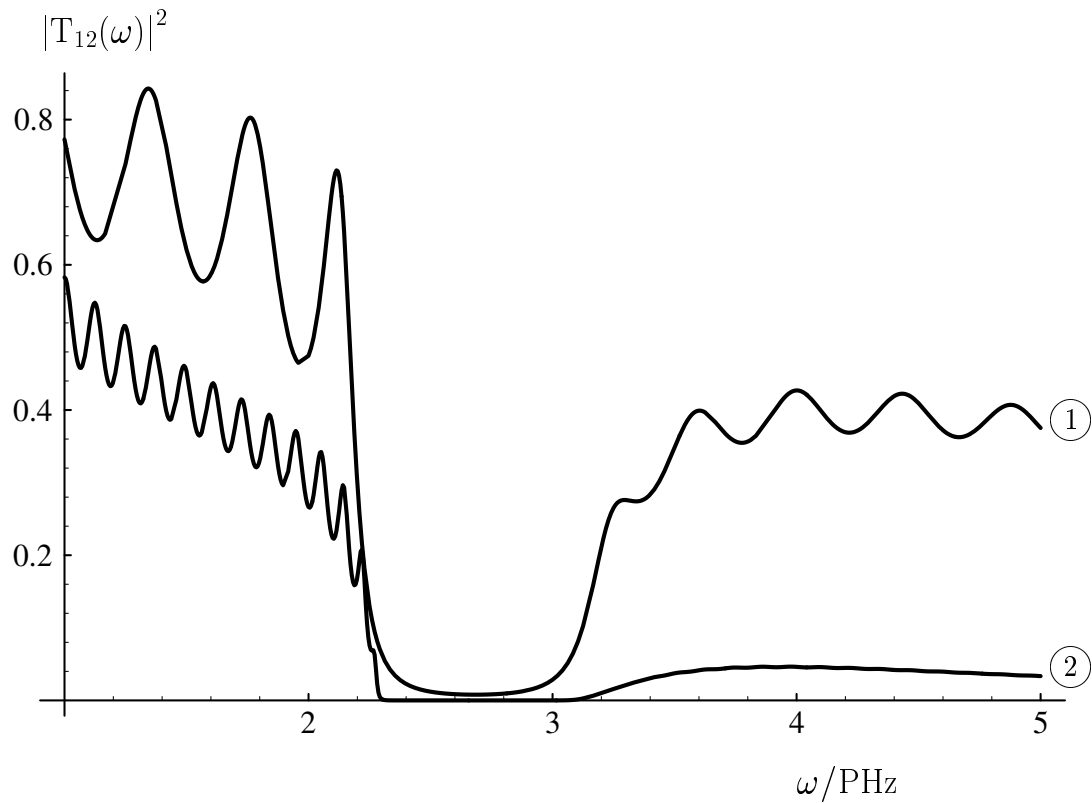


Figure 3: The square of the absolute value of the transmittance of a multilayer absorbing barrier,  $|T_{12}(\omega)|^2$ , is shown for  $N = 11$  layers [curve (1)] and  $N = 41$  layers [curve (2)]. The data are the same as in Fig. 2.

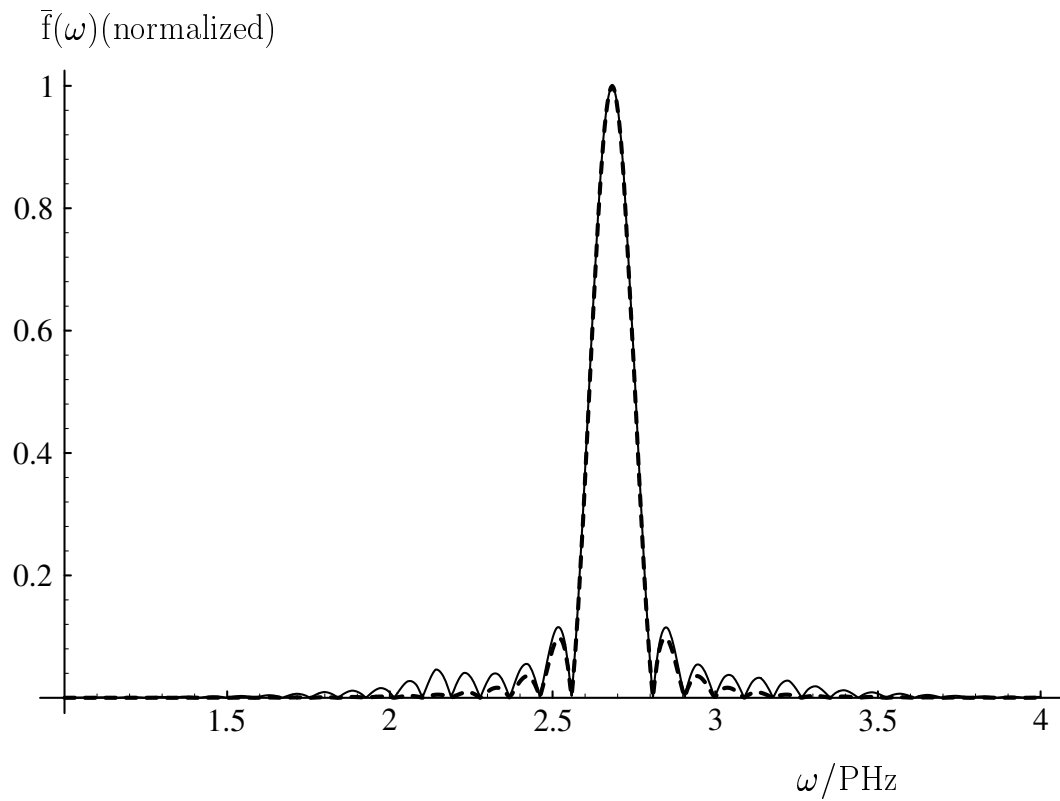


Figure 4: The (normalized) spectral line shape function  $\bar{f}(\omega)$  (full line) of a photon after having passed through an absorbing barrier consisting of  $N = 11$  layers (data as in Fig. 2) is shown. For comparison, the line shape function of the incoming pulse that is assumed to be limited in time ( $2t_0 = 40$  fs) is also shown (dashed line).

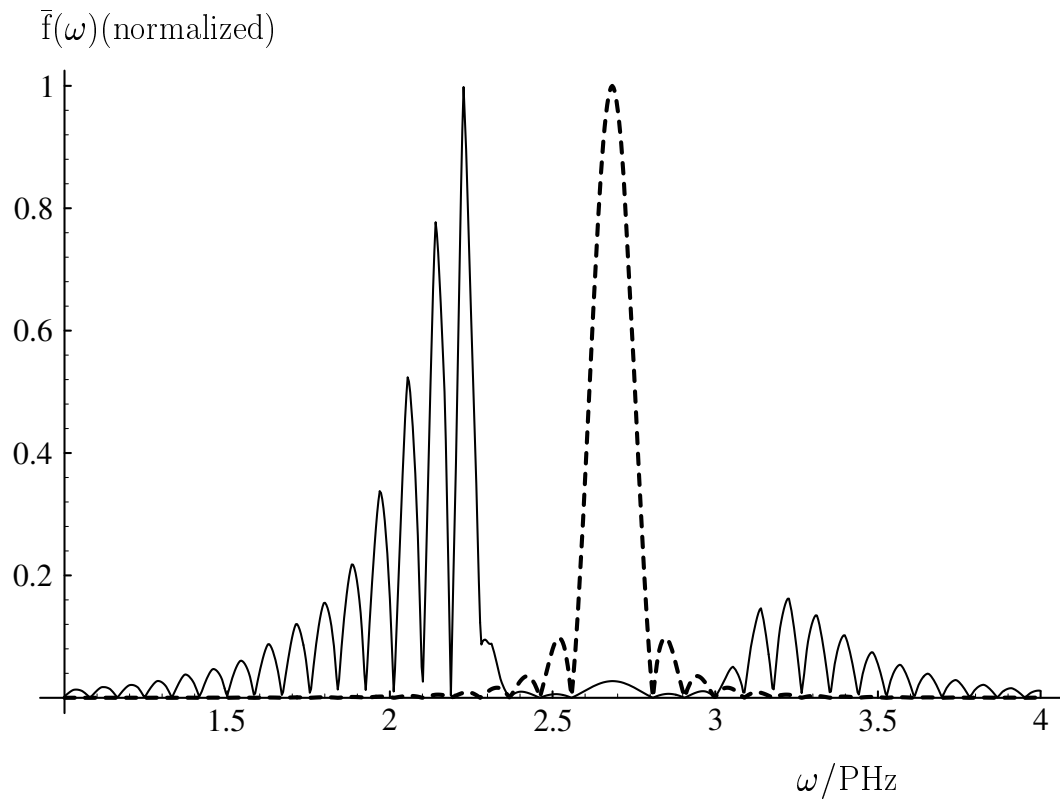


Figure 5: The (normalized) spectral line shape function  $\bar{f}(\omega)$  (full line) of a photon after having passed through an absorbing barrier consisting of  $N = 41$  layers (data as in Fig. 2) is shown. For comparison, the line shape function of the incoming pulse that is assumed to be limited in time ( $2t_0 = 40$  fs) is also shown (dashed line).

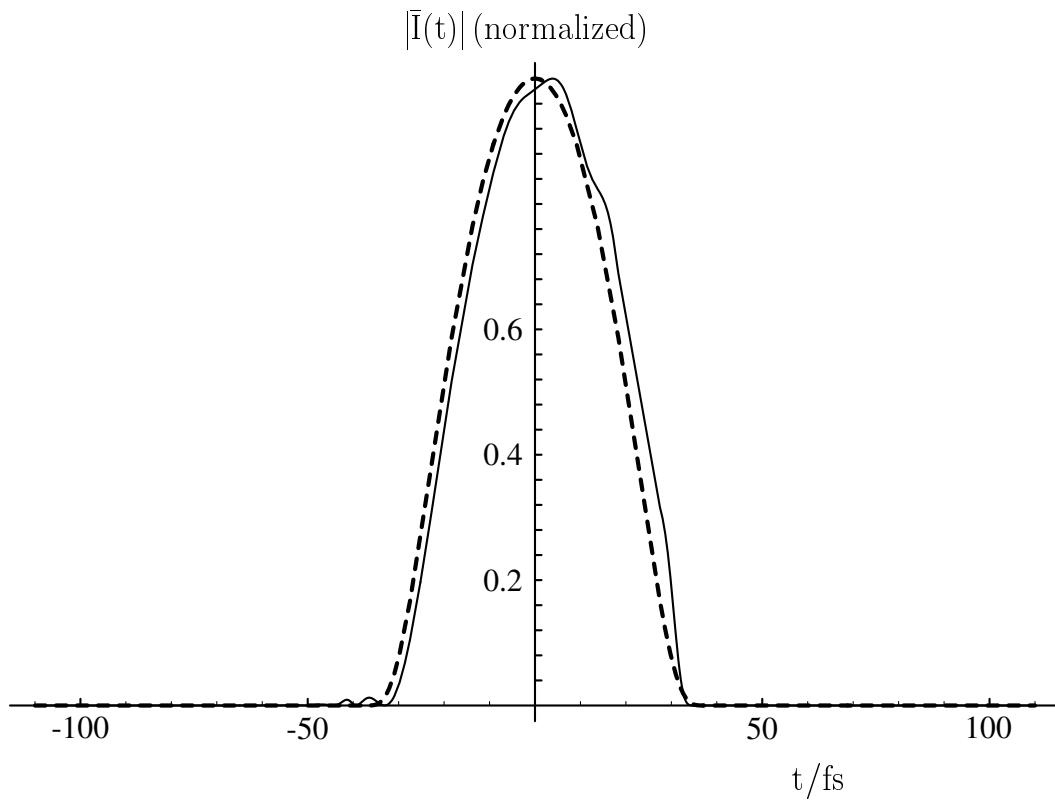


Figure 6: The (normalized) intensity  $\bar{I}(t)$  (full line) of a photon after having passed through an absorbing barrier consisting of  $N = 11$  layers (data as in Fig. 2) is shown. For comparison, the intensity of the incoming pulse that is assumed to be limited in time ( $2t_0 = 40$  fs) is also shown (dashed line).

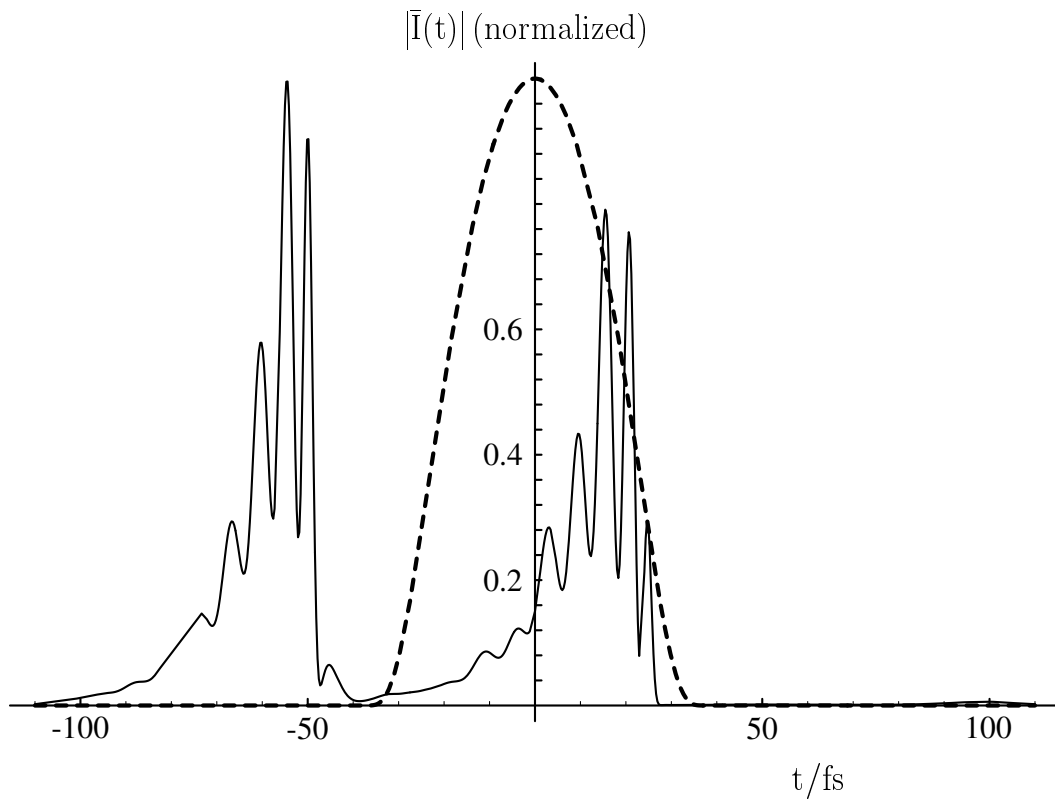


Figure 7: The (normalized) intensity  $\bar{I}(t)$  (full line) of a photon after having passed through an absorbing barrier consisting of  $N = 41$  layers (data as in Fig. 2) is shown. For comparison, the intensity of the incoming pulse that is assumed to be limited in time ( $2t_0 = 40$  fs) is also shown (dashed line).



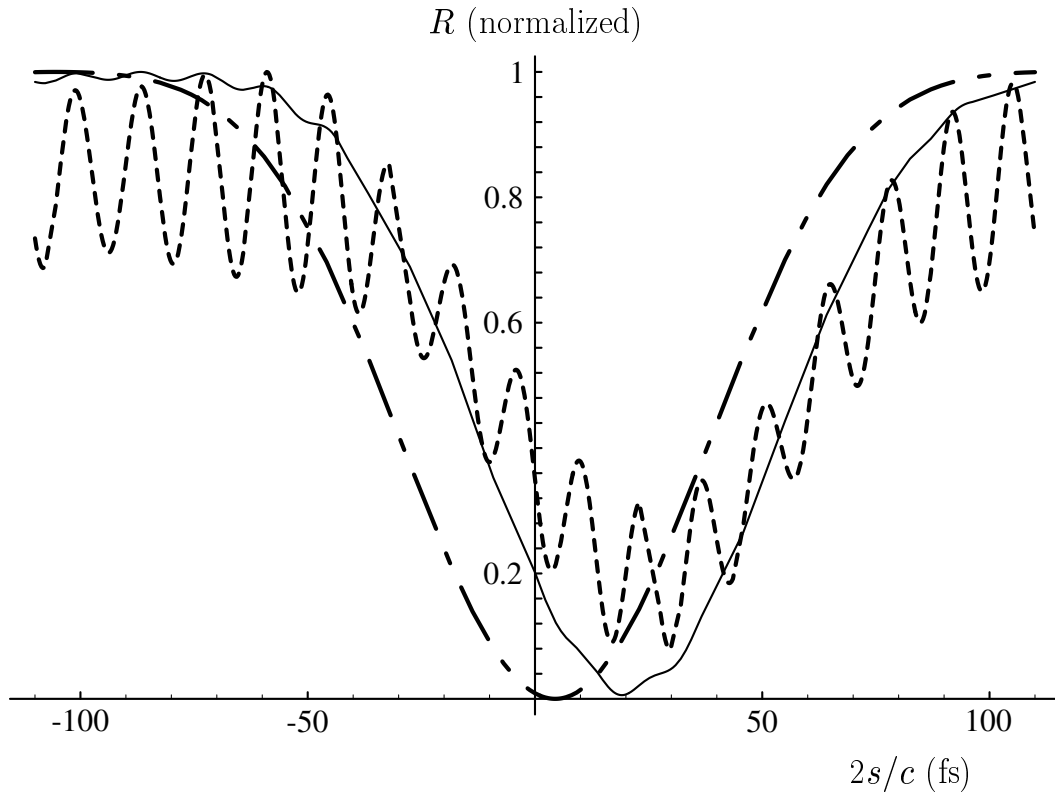


Figure 8: The (normalized) coincidences  $R(s)$  are shown in dependence on the translation length  $s$  for a time-limited pulse of the incoming photon ( $2t_0 = 40$  fs) and various numbers of the layers of a lossless barrier:  $N = 11$  (dotted-dashed line),  $N = 35$  (full line),  $N = 41$  (dashed line). The data of the lossless barrier are the same as in Fig. 2.

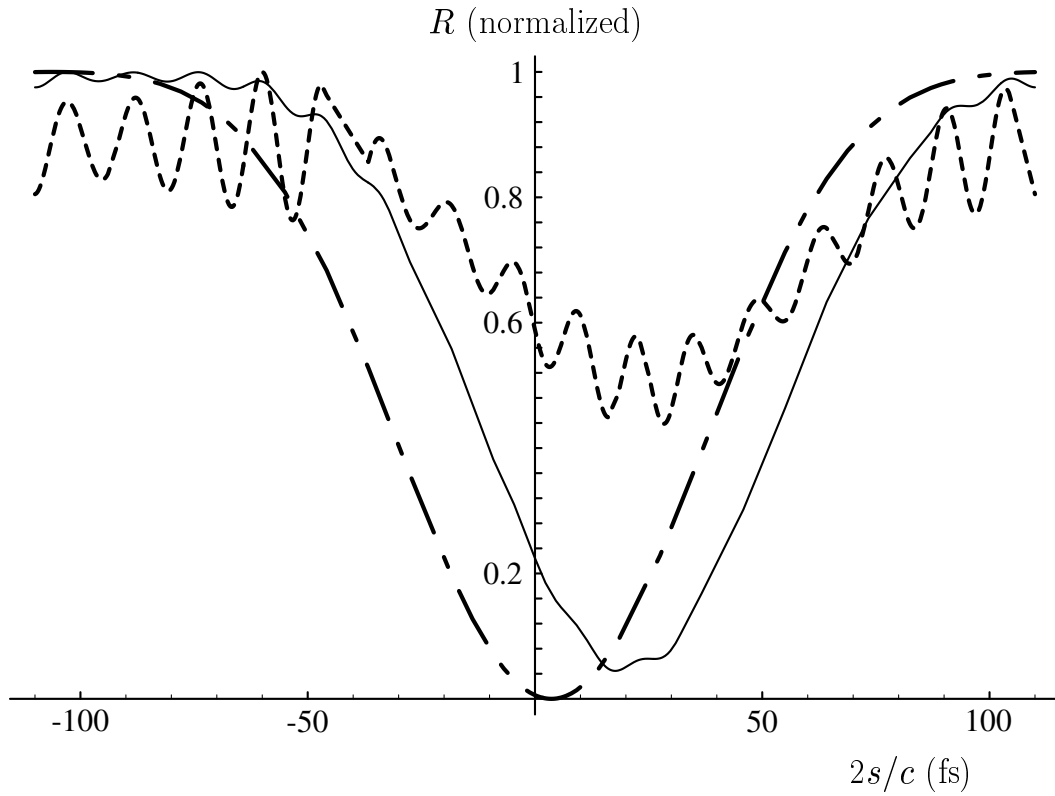


Figure 9: The (normalized) coincidences  $R(s)$  are shown in dependence on the translation length  $s$  for a time-limited pulse of the incoming photon ( $2t_0 = 40$  fs) and various numbers of the layers of an absorbing barrier:  $N = 11$  (dotted-dashed line),  $N = 41$  (full line),  $N = 49$  (dashed line). The data of the absorbing barrier are the same as in Fig. 2.